Experimental investigation on the influence of a multi-scratched shaft on hydrodynamic journal bearing performance

J. Bouyer, Y. Alexandre, M. Fillon

Experimental investigation on the influence of a multi-scratched shaft on hydrodynamic journal bearing performance.

J. Bouyer [1], Y. Alexandre [2], M. Fillon [1]

[1] *Pprime Institute, CNRS – University of Poitiers – ISAE ENSMA, UPR 3346, Mechanical Engineering and Complex Systems Dept., SP2MI, 11 Bd Marie & Pierre Curie, TSA 41123, 86073 Poitiers Cedex 9, France.*

[2] *LTDS, UMR 5513, École Centrale de Lyon, 36 Avenue Guy de Collongue, 69134 Ecully Cedex, France.*

Keywords: Experimental, scratches, journal-bearing performance

Abstract

Energy production machinery is one of the main subjects of current engineering research. Manufacturers and users are seeking to increase the performance of these machines and, thus, to extend the maintenance intervals as far as possible. It is therefore essential to predict their behavior according to their wear to schedule maintenance operations. This work aims to present data allowing the comparison of numerical results to physical behavior. The essential parameters of the bearing (temperature, pressure, friction) are measured, varying the operating conditions in terms of speed and load. Whatever the operating condition, scratches induce a strong modification of the pressure field, which is reduced close to zero in the zone facing the scratch. The most detrimental case is that with multiple scratches, which significantly reduces the load-carrying capacity of the bearing. In this case, the maximum pressure in the bearing mid-plane increases by more than 50% and the maximum temperature by more than 15 K.

Introduction

Improving the performance of energy production machinery is currently one of the leading subjects of engineering research. Whether in terms of production power or environmental impact, these devices are now the subject of much attention. Manufacturers and users are seeking to increase the performance of these machines and, thus, to extend the maintenance intervals as far as possible. It is therefore essential to predict their behavior according to their wear and tear to know when best to stop them for maintenance. This work aims to provide data to bearing users and/or researchers to allow them to evaluate the performance of their bearing as a function of its wear. Global parameters, such as friction torque, and local ones, such as pressure and temperature measurements, are presented and discussed as a function of the number of grooves and as a function of groove depth. After a short literature review, the materials and methods are presented before the results and their discussion.

A broad view of the literature on the effects of wear in lubricated contacts reveals two main fields of study: biology, with a great deal of work on joint prostheses for example, and mechanical engineering, with work focused more on power generation machines. Since the scope of the present

work is engineering, we will not extensively present the biological studies to be found in the literature. Nevertheless, we can cite that of Park *et al.* [1], who recently studied the influence of wear on the performance of metal-on-metal implants. They concluded that, even if there is a large range of in vivo wear rates within the same implant type, the implant design was the cause of the extensive wear. However, such papers are not so far from tribology, and studies accounting for the influence of third-body abrasion can be found in the same journals [2]. Going closer to engineering, some papers in the field of biotribolgy, such as Garabédian *et al* [3] are interested in the wear patterns caused by the presence of wear debris that are released in contact by the body. They showed that released metallic bone ingrowth beads, before being embedded in the PE component, are entrapped in the articulating interface, thus creating scratches on the PE Surface. Consequently, the embedded beads release a population of metallic debris that induce a large wear of the prosthesis. This study is close to what could be done in mechanical engineering, in a journal bearing for example, where metallic debris can cause several scratches at the shaft surface before being entrapped in the Babbitt.

Back to the mechanical engineering domain, the literature presents many works on journal bearing wear, which are often devoted to the study of wear appearance and its causes. This problem is also addressed in mechanical seals, but we will not discuss this here. Very few papers examine the scratches and their influence on bearing performance. One of the first to be found is that of Scherer [4] who studied wear in crankshaft bearings and ways of reducing this. He showed that large particles might cause scratches starting at the oil groove and spreading diagonally over the bearing surface but that surface erosion could also be caused by poor surface finish, corrosion, and cavitation. He proposed that the design of oilways and bearing alloys could be adapted to prevent such issues. Ten years later, Das and Dancer [5] published a book where they showed that crankshaft bearing performance was strongly dependent on the manufacturing tolerances and layouts of oil holes but also on machining and operating conditions. They showed that scratches could have highly detrimental effects. In 1994, Andersson *et al.* [6] studied an SiC water-lubricated bearing. They realized a series of journal bearing tests to evaluate the wear characteristics of SiC materials in repeated start-up events in which the lubrication conditions move from direct contact to hydrodynamic, thus proving that SiC-based materials could be utilized for water-lubrication. About ten years later, Branagan [7, 8] performed the first study (to our knowledge) dedicated to scratches with a simplified short bearing approach to characterize the influence of scratch depth on the load capacity of the bearing. He showed that a deep scratch could generate an up to 75% loss in load capacity and that the scratch significantly influences the temperature of the oil film. More recently, Keskin and Aydin [9] studied the failures of a crankshaft made of nodular graphite cast iron in a gasoline engine. The main reason for failure was determined as thermal fatigue due to contact of the surfaces generated by the presence of cracks and their growth but also by scratches on the journal's surfaces. The first study on the influence of scratches on the performance of bearings is that of Dobrica and Fillon [10], who conducted a numerical study on performance degradation in scratched journal bearings. They performed a parametric study to determine the influence of depth, extent of the scratched region, and density and position of the scratches independently. They identified critical scratch configurations that can lead to bearing damage. Hélène et al. [11] proposed a new study in 2013 on the influence of the geometrical parameters of the scratch on the performance of a journal bearing. They showed that even very shallow scratches have an impact on the bearing health and that the influence depends not only on the geometry but also on the position of the scratch. In the same period, Branagan [12] published a survey on damaged bearings where he collected several analyses to understand the sources and consequences of damage on Babbitted industrial bearings, both hydrodynamic and hydrostatic. Giraudeau *et al.* [13] also numerically evaluated the influence of several scratch parameters (depth, extent, density, etc.) for a two-lobe journal bearing. Most of the parameters had significant and straightforward impacts on bearing performance. Bouyer *et al.* [14]

continued this study by performing numerical/experimental comparisons with a numerical code based on that developed in [10], taking into account thermal effects and coupled with FEM calculation for the deformations. The obtained TEHD solutions were compared to experimental data for a wide range of operating conditions and proved to have a good agreement. More recently, Ranjan *et al.* [15] integrated the analysis of wear debris, vibration, and temperature of journal bearings in a hydropower plant fault diagnosis. They observed an abnormal increase in temperature after 200 days of continuous operations and noticed scratches and wiping marks over the surface of the bearing block and side thrust pad, proof of the bearings losing load capacity.

As shown in this short literature review, only a few works study the influence of scratches on the performance of journal bearings. The aim of this work is thus to present comparison data for researchers' numerical results. The essential parameters of the bearing (temperature, pressure, film thickness) were measured, varying the operating conditions in terms of speed and load. The next section will present a short description of the test rig.

Materials and Methods

Test Rig

The test rig used in this study is the journal bearings test rig at the Pprime Institute. This test rig has been used for numerous experiments on both fixed geometry and tilting-pad journal bearings over the past forty years. Consequently, we provide only a brief reminder of its capacities and the details of its instrumentation, which are very well detailed in reference [13].

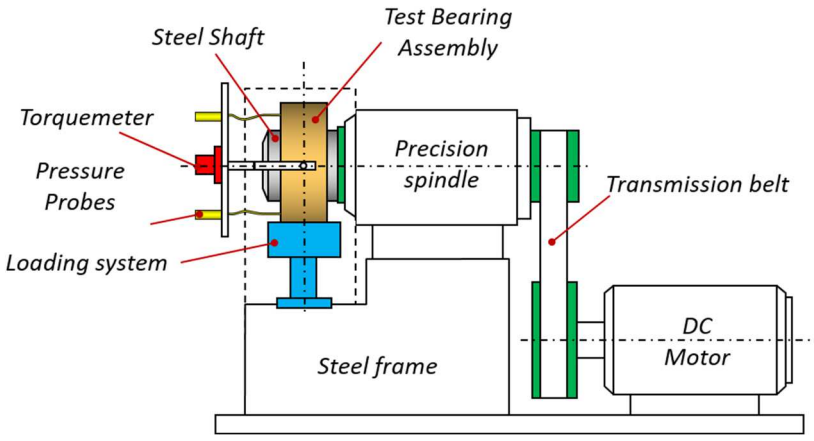

Figure 1. Schematic view of the test rig

Figure 1 shows a schematic view of the test rig. It is composed of a precision spindle driven by a 21 kW motor using a flat belt. The maximum speed is 12,000 rpm. The test cell comprising the shaft and housing is placed in front of the test rig to allow easy replacement of the parts. A double hydrostatic bearing transmits the load to the housing without any friction with values up to 10,000 N. A torque meter directly measures the friction induced by hydrodynamic forces in the fluid film. A hydraulic system controls both feeding pressure and feeding temperature to be constant in all tests by means of a PID Controller. Supply oil was ISO VG 46 and its temperature was maintained at 45°C± 0.5°C at a constant pressure of 0.17 MPa. The journal bearing geometrical parameters and the lubricant properties are given in Table 1. The bearing is the same as that in [13], a two-lobe bearing with a 0.524 clearance ratio. Table 2 gives an overview of the uncertainties of the different probes used in this study. It has to be noted that each operating point (fixed load and speed) was repeated at least 3 times in order to ensure a good repeatability. The results presented here as thus obtained

from an averaged value of the 3 tests. The maximum discrepancies for the temperature measurements were less than 0.5 K, 2% for the pressure and 1% for the friction torque.

Parameter	Symbol	Value
Bearing diameter	D	100 mm
Shaft diameter	d	99.772 mm
Bearing length	L	68.4 mm
Horizontal radial clearance	C	143 µm
Vertical radial clearance	C_b	68 µm
Preload ratio	m	0.524
Lubricant	-	ISO VG 46
Supply temperature	T_s	45°C
Supply pressure	p_s	0.17 MPa
Density	ρ	850 $kg.m^{-3}$
Dynamic viscosity at 40°C	μ_{40}	0.0416 Pa.s
Dynamic viscosity at 60°C	μ_{60}	0.0191 Pa.s

Table 1. Bearing and lubricant characteristics

Measurement	Uncertainty
Speed	±10 rpm
Load	±10 N
Relative film thickness	± 1 µm
Friction torque	± 0.05 N.m
Temperature	± 0.5 K
Pressure	± 0.3% of range scale
Flow rate	± 0.05 l/min

Table 2. Measurement uncertainties

Bearing housing

The instrumentation for the bearing is composed of 20 type K thermocouples and 18 pressure measurements placed at strategic positions, plus additional peripheral temperature measurements. Figure 2 shows the placement detail of the probes on the housing. Figure 2 presents the spatial repartition of pressure and temperature probes. The vertical axis represents the axial coordinate, 0 is the front section and 68.4 the back section of the bearing. The circumferential coordinate is the abscissa; 0° is at the top of the bearing. The supply grooves (yellow rectangles) are placed at ± 90° from the load direction. The loaded lobe (between 107.5 and 247.5°) is the most equipped one. Again, for all details about bearing or test rig equipment, please refer to [13].

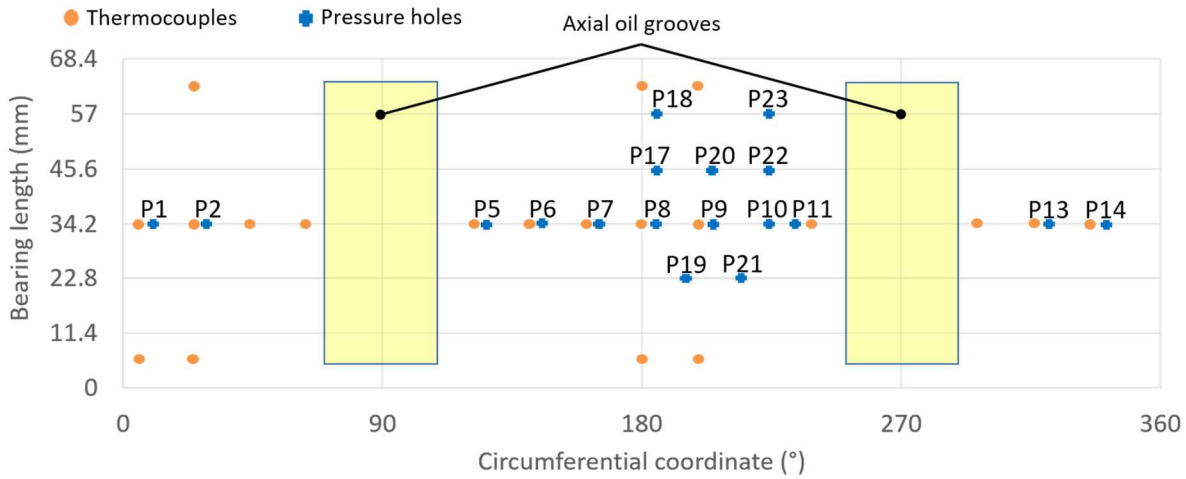

Figure 2. Bearing equipment

Shaft

The shaft is the main component that differs from the previous studies. Indeed, previous work [10] showed that the presence of a scratch significantly influences the shape of the pressure field. The depth of the scratch has also a strong influence; the deeper the scratch, the higher the modification of pressure as soon as its depth is greater than the clearance C. At high eccentricity, i.e. when the applied load is high and the rotational speed is low, this effect is even more visible. When compared to numerical simulations in [13], experiments also showed that the spherical hydrostatic bearing that is used on the test rig allowed creating a slight misalignment in the single scratch cases, created by the dissymmetry of the pressure field. To avoid this problem, it was decided to create only symmetric scratches in this study. Hence, the experiments presented in this paper can be classified as a function of the shaft geometry with or without scratches. The following configurations were tested:

1. No scratch,
2. 2 scratches located at L/3 and 2L/3 axial coordinates (22.8 and 45.6 mm respectively),
3. 2 scratches located at 5L/12 and 7L/12 axial coordinates (28.5 and 39.9 mm respectively),
4. Multi-scratch shaft with 16 scratches, varying from 55 to 330 µm in depth.

A Taylor Hobson CCI was used to measure the geometrical profile of the shaft. The resolution along z axis of this device is less than 0.1µm. The measurement technique was the following: three scratch depth measurements were performed at different circumferential positions and averaged to obtain a mean value. Those three measurements were repeated two times at different days and the final value of the scratch depth was then issued from 9 measurements. Figure 3 presents a typical measurement that was taken on the shaft with 2 scratches at 5L/12 and 7L/12 axial coordinates. It must be noted that some zones have been removed to avoid any artifacts due to the imprecision of the measurements at the boundaries. Orange highlights represent the zones that were chosen to proceed to depth evaluation. Considering these measurements, the average depth of the 5L/12 and 7L/12 were respectively 254 and 247 µm. The multi-scratch bearing was measured following the same modus operandi. An example measurement is given in Fig. 4. Different scratch depths are clearly visible and, as can be seen in the table below the graph of Figure 4, the mean depths vary from 50 to 300 µm. This result was obtained by subtracting 35 µm from the values, corresponding to the plane 1 Z mean, which is supposed to be zero.

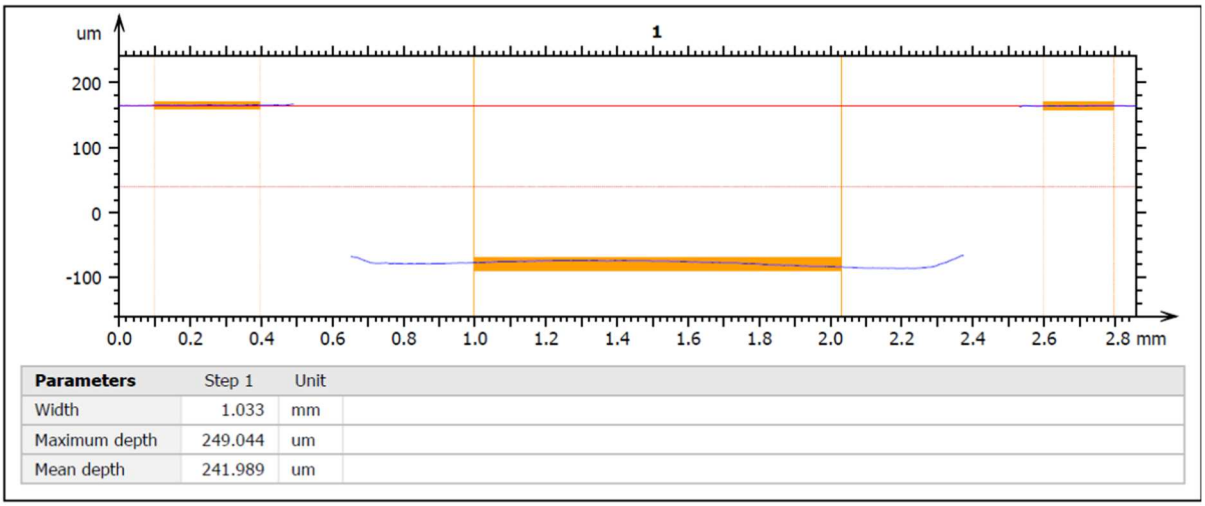

Parameters	Step 1	Unit
Width	1.033	mm
Maximum depth	249.044	um
Mean depth	241.989	um

Figure 3. Depth typical measurement for the 7L/12 scratch.

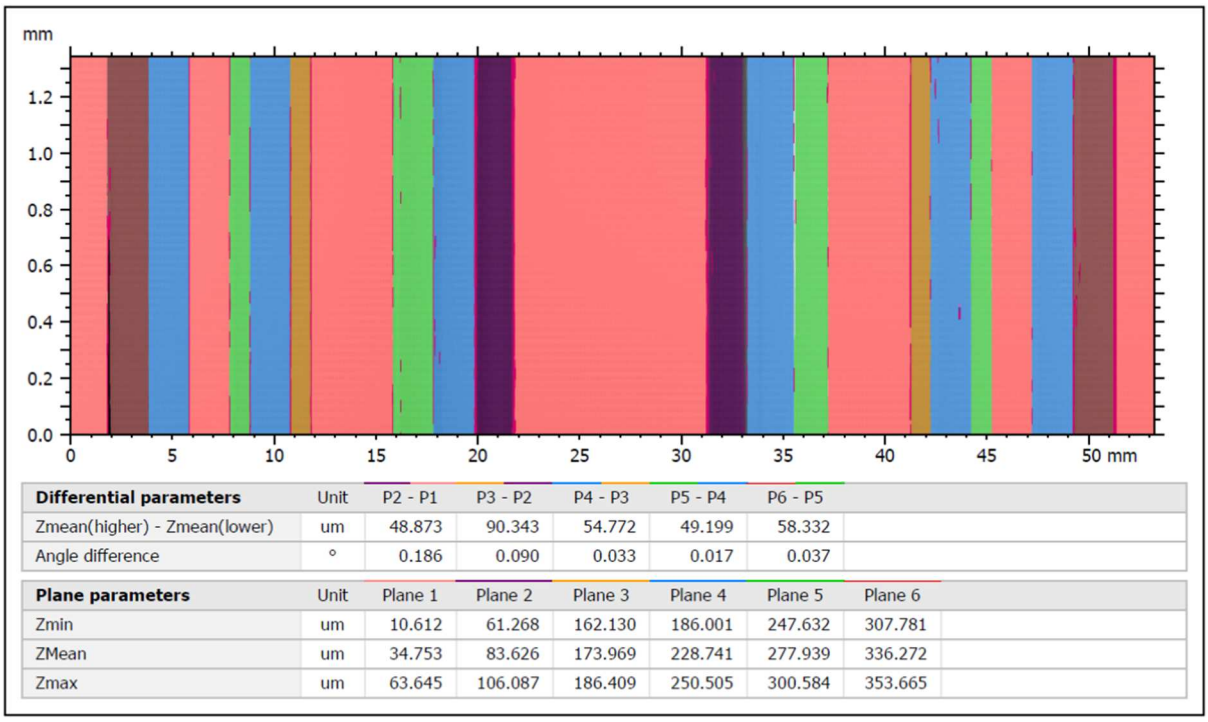

Differential parameters	Unit	P2 - P1	P3 - P2	P4 - P3	P5 - P4	P6 - P5
Zmean(higher) - Zmean(lower)	um	48.873	90.343	54.772	49.199	58.332
Angle difference	°	0.186	0.090	0.033	0.017	0.037

Plane parameters	Unit	Plane 1	Plane 2	Plane 3	Plane 4	Plane 5	Plane 6
Zmin	um	10.612	61.268	162.130	186.001	247.632	307.781
ZMean	um	34.753	83.626	173.969	228.741	277.939	336.272
Zmax	um	63.645	106.087	186.409	250.505	300.584	353.665

Figure 4. Scratch depth measurements on the multi-scratch shaft.

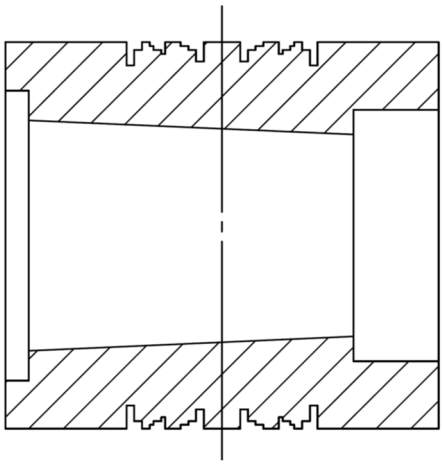

Figure 5. Schematic view of the shaft design

Fig. 5 is the drawing that was used to manufacture the shaft scratches. It comprised 16 scratches distributed symmetrically to the bearing mid-plane. Beginning from the front of the bearing at 0 axial coordinates, the first scratch is located at L/6 (11.4 mm) and has a depth of 300 µm. The location and depth of the 16 scratches whose detailed profiles are presented by Fig. 6 are given in Table 2. As described before, we can see here that the shaft has four deep scratches located at L/6, 5L/12, 7L/12, and 5L/6 axial coordinates, with a depth of approximately either 250 or 300 µm.

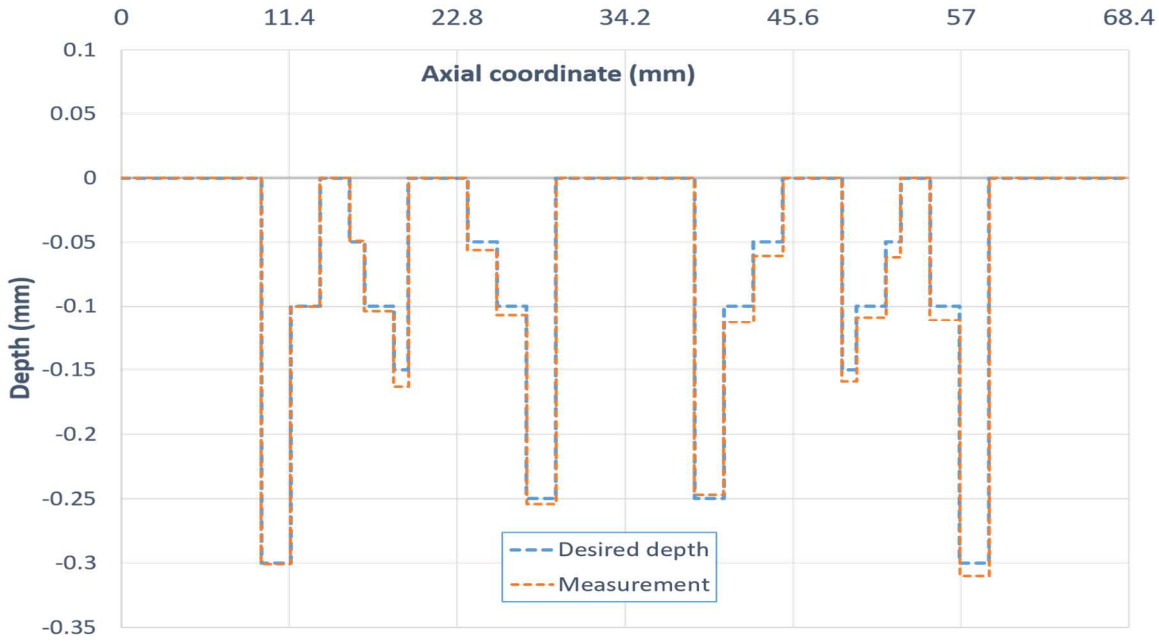

Figure 6. Comparison between desired and real depths.

Axial Coordinate (mm)	Desired Depth (µm)	Measured Depth (µm)	Axial Coordinate (mm)	Desired Depth (µm)	Measured Depth (µm)
0–9.5	0	0	34.2–38.9	0	0
9.5–11.5	300	301	38.9–40.9	250	247
11.5–13.5	100	100	40.9–42.9	100	113
13.5–15.5	0	0	42.9–44.9	50	61

15.5–16.5	50	49	44.9–48.9	0	0
16.5–18.5	100	104	48.9–49.9	150	159
18.5–19.5	150	163	49.9–51.9	100	109
19.5–23.5	0	0	51.9–52.9	50	62
23.5–25.5	50	56	52.9–54.9	0	0
25.5–27.5	100	107	54.9–56.9	100	111
27.5–29.5	250	254	56.9–58.9	300	310
29.5–34.2	0	0	58.9–68.4	0	0

Table 2. Desired and measured scratch depths on the test shaft

Experimental results and discussion

The results presented here include only part of the conditions that were tested over all the test campaigns. Overall tests were performed for speeds ranging between 500 and 8,000 rpm and loads between 500 and 10,000 N. Not all combinations were possible due to dangerous operating conditions reached when eccentricity was too high. To maximize the effects and the differences between cases, we first present only results for 3,500 rpm and the highest load of 8,000 N. To emphasize the thermal effects, the results obtained on the multi-scratch bearing at 8,000 rpm are also presented for loads between 500 and 5,000 N. As shown in previous work [9, 10], the most significant influence of scratches on the bearing performance acts on the pressure field. The differences in temperatures are weaker and the behavior remains predictable with a simple global increase in temperature with speed.

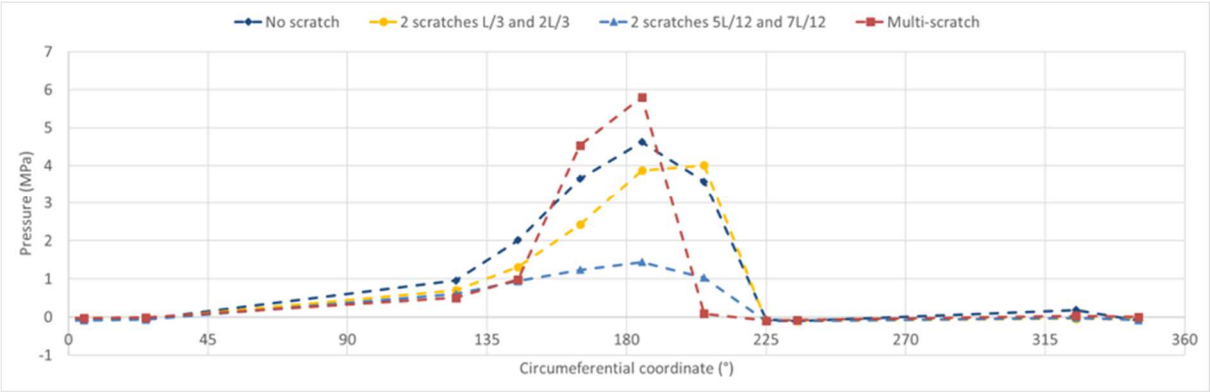

Figure 7. Circumferential hydrodynamic pressure at the bearing mid-plane for different scratch configurations at 3,500 rpm and 8,000 N.

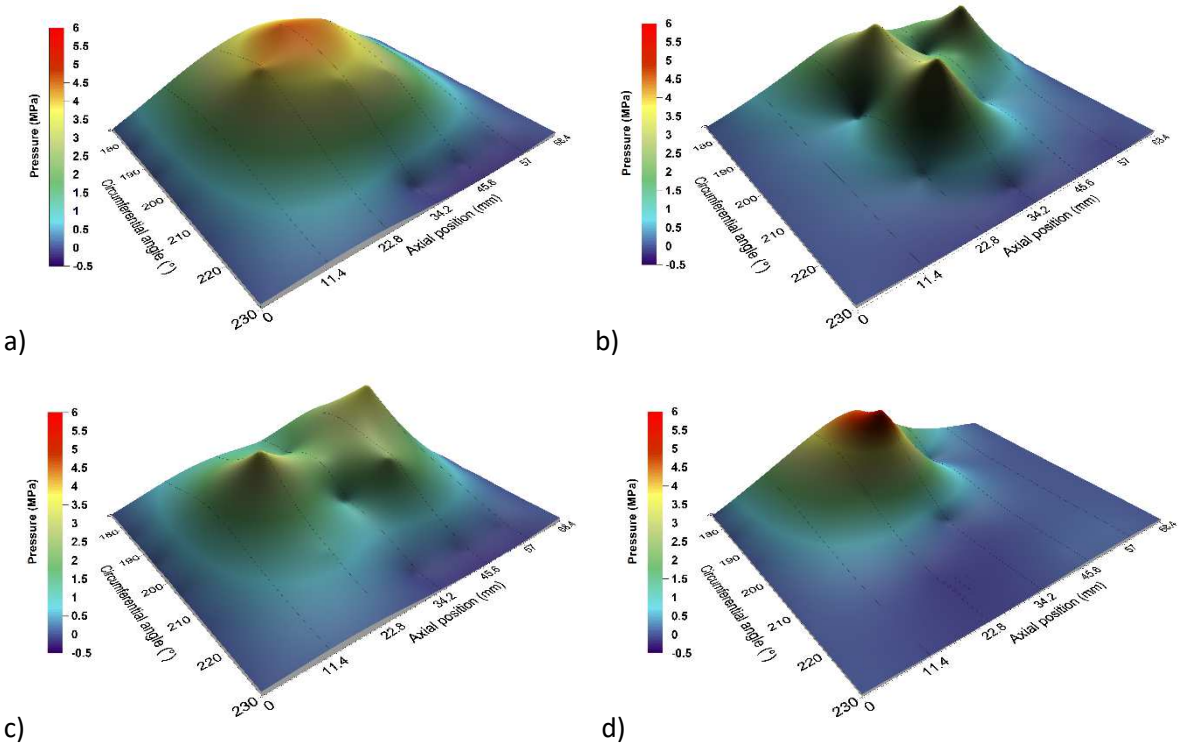

Figure 8. Pressure map representation between 175 and 225° (loaded lobe). a) No scratch. b) 2 scratches at L/3 and 2L/3. c) 2 scratches at 5L/12 and 7L/12. d) Multiple scratches.

Figure 7 shows the hydrodynamic pressure measured in the bearing mid-plane at 3,500 rpm and 8,000 N for the four configurations with no scratch, two scratches at L/3 and 2L/3, two scratches at 5L/12 and 7/12, and multi-scratch. Figure 8 gives a representation of the pressure field in the high-pressure region for the same four cases. Those pressure zooms are obtained from the data given by probes P7, P8, P9, P10, P11, P17, P18, P19, P20, P21, P22, and P23 at angular coordinates between 175 and 230° and axial positions between 22.8 and 57 mm, as shown in Fig.2. For better understanding, Figures 7 and 8 are discussed together. The influence of scratches on pressure is clearly visible in Fig. 7, where the maximum pressure appears to be decreased when 2 scratches are made on the shaft. For the L/3 and 2L/3 configuration, the maximum pressure in the bearing mid-plane is increased but was not caught by the probes because of their location. The maximum recorded pressure is located at 195° with a 15%decrease, as shown in Fig. 8b, and the pressures at the location of the scratches are recorded as 0. The maximum pressure being at 185° for the unscratched configuration probably moves towards a downstream value between 185 and 195°. The explanation is different for the 5L12 and 7/12 configuration. First, a strong decrease is observed, the maximum pressure is reduced by 70% and its location remains at 185°. This is because the scratches are very close to the bearing mid-plane and each other. Indeed, the unscratched zone facing the probes in the mid-plane is very narrow and does not permit building a high pressure, being moved to both sides of the bearing as the pressure measurements plotted in Fig. 8c show. Concerning the pressure field for the multi-scratch bearing, the unscratched region in the bearing mid-plane is still narrow but, due to the presence of the numerous scratches, it remains one of the only regions where it is possible to build pressure to sustain the load. The pressure in this zone is consequently much higher than in the unscratched case, with an increase of 25%.

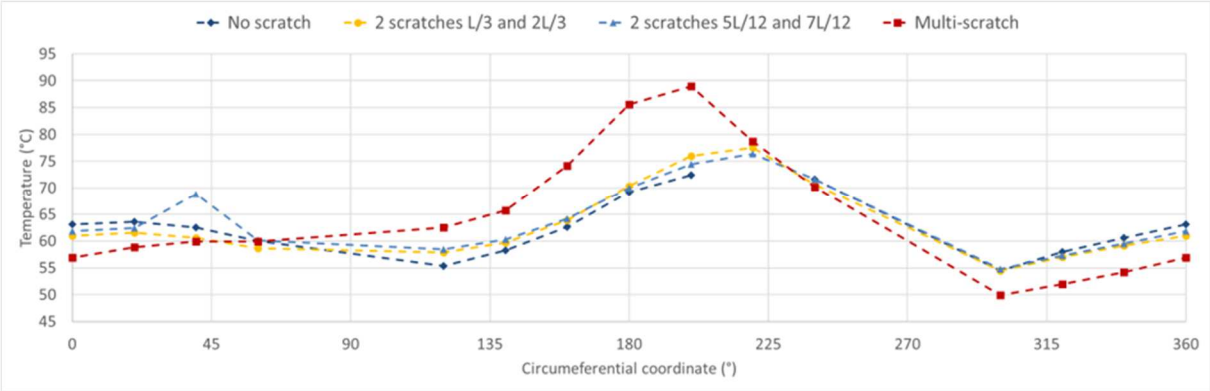

Figure 9. Circumferential temperature at the bearing mid-plane for different scratch configurations at 3,500 rpm and 8,000 N.

As mentioned before, the presence of two scratches barely affects the shape and values of the temperature field in the bearing mid-plane (Fig. 9) compared to the bearing with no scratch. Nevertheless, an increase of 15 K in the maximum temperature zone was observed for the multi-scratch bearing due to the high decrease in film thickness corresponding to the strong increase in pressure. At the opposite, in the upper zone of the bearing (from -60° to +30°), where the film thickness is higher (due to a higher shaft eccentricity), the temperature of the multi-scratch bearing is 5 K lower the temperature of the three other configurations. As can be seen in Fig. 10, the axial temperature profile does not change but an increase in temperature occurs in the mid-plane and a global temperature increase is also noticed. Indeed, the temperature increases on both bearing ends, 9 K in the front section and 11 K in the back section. This shows that the temperature field is not symmetrical but the difference between front and back sections remains lower than 2 K. This phenomenon is because the front section is completely opened to ambient whereas the back section faces the spindle of the test rig, which provides thermal radiation.

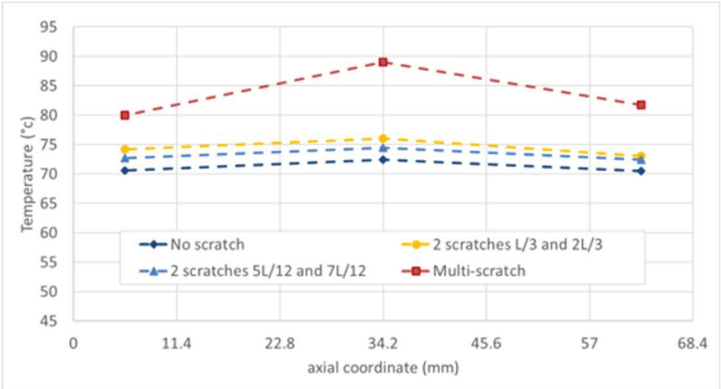

Figure 10. Axial temperature at 200° for different scratch configurations at 3,500 rpm and 8,000 N.

Concerning the friction torque and the axial flow rate that are global parameters, the values are presented in Table 3 for the four bearing configurations. Compared to the unscratched bearing, the presence of two scratches induces the torque to increase between 8 and 10%, whereas, for the multi-scratch bearing, the increase reaches more than 25%. The variation of the flow rate is opposite, it being reduced by more than 8% for the 2 scratches cases and 18% for the multi-scratch configuration compared to the unscratched case. This behavior is mainly due to the increase of the shaft eccentricity, i.e. a smaller film thickness. The shear is significantly increased, thus leading to a higher friction torque. Moreover, even if the inlet flow rate increases due to the presence of the scratches, the axial flow rate decreases because of the higher recirculation flow (circumferential)

from one lobe to the following one. Those results prove that the load-carrying capacity of the multi-scratch bearing is significantly reduced.

Bearing configuration	Friction torque (N.m)	Axail flow rate (l/min)
No scratch	3.70	4.75
2 scratches L/3 and 2L/3	4.05	4.47
2 scratches 5L/12 and 7L/12	3.99	4.40
Multi-scratch	4.70	3.91

Table 3. Hydrodynamic friction torque under steady-state conditions: 3,500 rpm and 8,000 N.

To develop the thermal effects, the next discussion will be on the multi-scratch bearing operating at 8,000 rpm. Several values of the load are presented without exceeding 5,000 N because of the dangerousness of higher loads. Figure 11 gives the pressures recorded in the bearing mid-plane for several loads at 8,000 rpm. Since the speed was very high, the bearing eccentricity was small under light loads up to 3,000 N. The shape of the pressure field only changes at 4,000 N, where the maximum pressure probably moves downstream to the 180° coordinate, as we discussed previously.

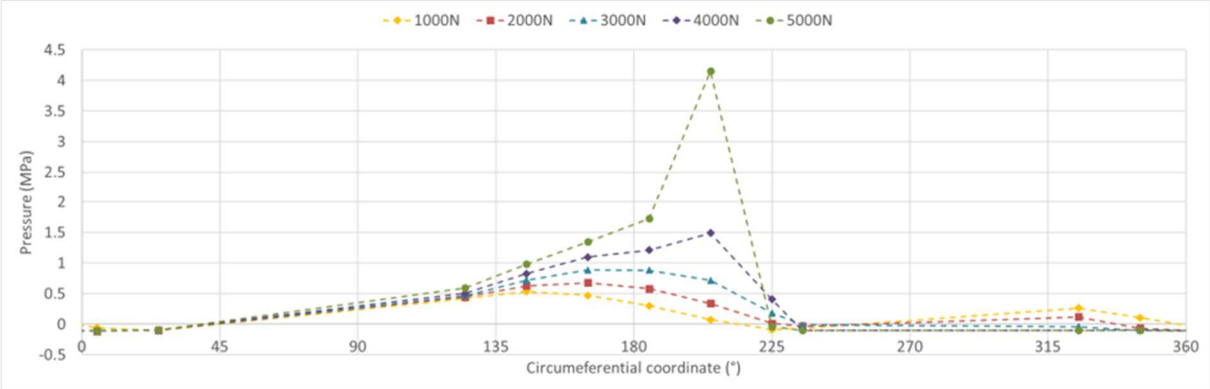

Figure 11. Circumferential hydrodynamic pressure at the bearing mid-plane for different loads at 8,000 rpm, multi-scratch bearing.

Figure 12 shows that the maximum temperature also moves downstream with increasing pressure. However, the major difference is visible in Fig. 13, where the behavior differs as a function of load. For light loads of 1,000 and 2,000 N, the maximum axial temperature was observed on both bearing ends. The eccentricity being low, the pressure buildup is the same at the bearing ends and in the center because they have the same functional surface (i.e. 9.5 mm, see Fig. 2. The temperature variation is thus only 2 or 3 K axially. For higher loads, the maximum temperature moves towards the center, and the difference reaches more than 5 K. This effect is due to the larger eccentricity and to the fact that both bearing ends are connected to the ambient pressure; they cannot develop high pressures. The development of high pressure is, therefore, possible only in the central part of the bearing, creating a sharp temperature increase in this zone.

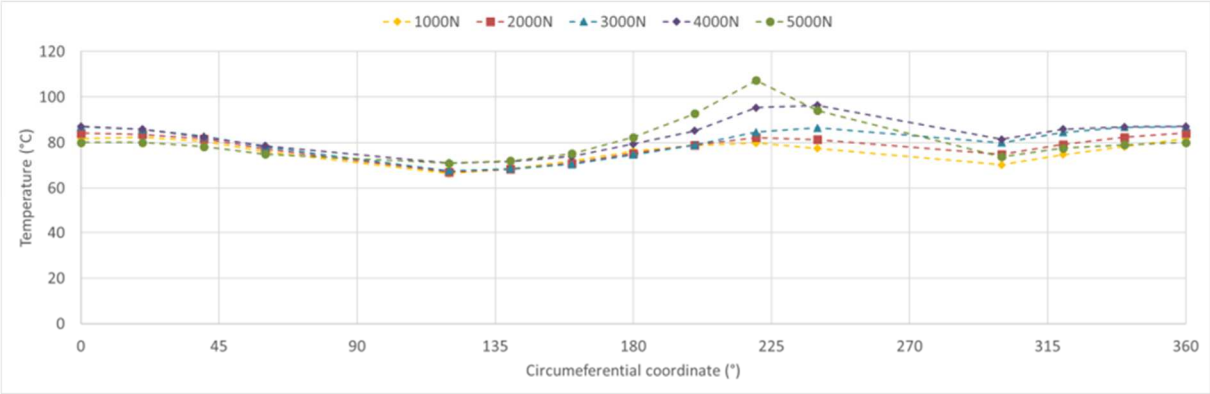

Figure 12. Circumferential temperature at the bearing mid-plane for different loads at 8,000 rpm, multi-scratch bearing.

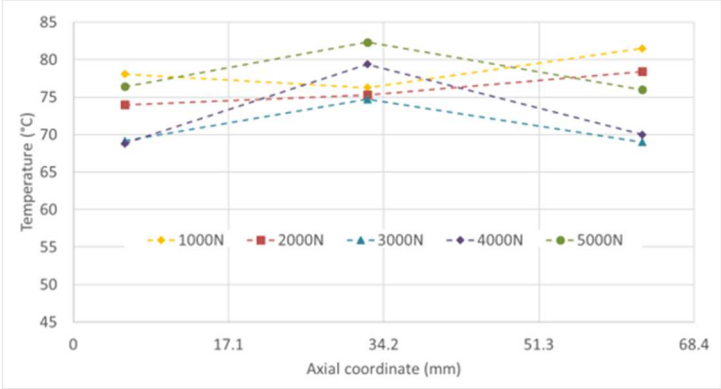

Figure 13. Axial temperature at the bearing mid-plane for different loads at 8,000 rpm, multi-scratch bearing.

Conclusions

This work concludes a series of 3 papers on the influence of scratches on hydrodynamic journal bearing performance. Different positions of deep scratches were compared, and the number of scratches was also studied.

This study confirms that scratches induce a strong modification of the pressure field that cannot develop over the full bearing length, the pressure being reduced close to zero in the zone facing the scratch. The maximum pressure moves downstream, and the multi-scratch bearing was found to have much lower performance than the unscratched one. The maximum pressure in the bearing mid-plane can be increased by more than 50%. The circumferential shape of the temperature field is barely modified, but the maximum temperature is increased by more than 15 K for the multi-scratch bearing while, at the same time and due to a higher shaft eccentricity, the minimum temperature is reduced by a few K in the thicker fluid film zone.

Future work will develop a complete TEHD model, taking into account the influence of scratches to be compared to the experimental data presented here, those being obtained with a fully known scratched shaft geometry.

References

[1] Park, S.-H., Lu, Z., Hastings, R.S., Campbell, P.A., Ebramzadeh, E. Five Hundred Fifty-five Retrieved Metal-on-metal Hip Replacements of a Single Design Show a Wide Range of Wear, Surface Features,

and Histopathologic Reactions. Clinical Orthopaedics and Related Research 2018. Vol. 476(2): 261–278. DOI: 10.1007/s11999.0000000000000044
[2] Clarke, I.C., Lazennec, J., Brusson, A. et al. Risk of Impingement and Third-body Abrasion With 28-mm Metal-on-metal Bearings. Clinical Orthopaedics and Related Research 2014. Vol 472: 497–508. DOI: 10.1007/s11999-013-3399-3
[3] Garabédian, C., Bigerelle, M., Najjar, D., Migaud, H. Wear Pattern on a Retrieved Total Knee Replacement: The "Fourth Body Abrasion". Biotribology 2017. Vol. 11: 29–43. DOI: 10.1016/j.biotri.2017.05.003
[4] Scherer, L. Study and Operating Conditions of Bearing Liners, Bearings, and Crankshafts. Energie Fluide 1973, Vol. 12(60): 73–79.
[5] Das, P.K., Dancer, S.B. The effects of common variations in diesel engine bearings. SAE International Conference 1983, Milwaukee. DOI: 10.4271/831286
[6] Andersson P., Nikkila A-P., Lintulab P. Wear Characteristics of Water-Lubricated SiC Journal Bearings in Intermittent Motion. Wear 1994. Vol. 179(1–2): 57-62. DOI: 10.1016/0043-1648(94)90219-4
[7] Branagan, L.A. Influence of Deep, Continuous Circumferential Scratches on Radial Fluid film Bearings. In proc. of 61st STLE Annual Meeting & Exhibition 2006, May 7-11, Calgary, Canada.
[8] Branagan, L.A. Toward a Quantitative Analysis of Journal and Bearing Scratches. Proceedings of the 5th EDF & LMS Poitiers Workshop 2006, October 5, Poitiers, France.
[9] Keskin, A.a, Aydin, K. Crack Analysis of a Gasoline Engine Crankshaft. Gazi University Journal of Science 2010, Vol. 23(4): 487–492.
[10] Dobrica M.B., Fillon M. Performance Degradation in Scratched Journal Bearings. Tribology International 2012, Vol. 51: 1-10. DOI: 10.1016/j.triboint.2012.02.003
[11] Hélène M., Beaurain J., Raud X., Fillon M. Impact of Scratches in Tilting Pad Journal Bearings – Influence of the Geometrical Characteristics of Scratches. Proceedings of the 12th EDF/Pprime Workshop 2013, September 17-18, Poitiers, France.
[12] Branagan, L.A. Survey of Damage Investigation of Babbitted Industrial Bearings. Lubricants 2014. Vol. 2: 1-21. DOI: 10.3390/lubricants3020091
[13] Giraudeau C., Bouyer J., Fillon M. et al. Experimental Study of the Influence of Scratches on the Performance of a Two-Lobe Journal Bearing. Tribology Transactions 2017, Vol. 60 (5): 942-955. DOI: 10.1080/10402004.2016.1238528
[14] Bouyer J., Fillon M., Helene M. et al. Behavior of a Two-Lobe Journal Bearing with a Scratched Shaft: Comparison between Theory and Experiment. Journal of Tribology 2019, Vol. 141 (2): 021702. DOI 10.1115/1.4041363
[15] Ranjan R., Ghosh S., Kumar M. Fault Diagnosis of Journal Bearing in a Hydropower Plant Using Wear Debris, Vibration, and Temperature Analysis: A Case Study. Proceedings of the Institution of Mechanical Engineers, Part E: Journal of Process Mechanical Engineering 2020, article in press. DOI: 10.1177/0954408920910290